QUALITATIVE THEORY OF DYNAMICAL SYSTEMS **4**, 425–438 (2004)
ARTICLE NO. 70

Some Remarks on the Dynamics of the Mixmaster Universe

Mark Pollicott

Department of Mathematics, The University of Manchester,
Oxford Road M13 9PL Manchester, England
E-mail: mp@ma.man.ac.uk

and

Howard Weiss*

Department of Mathematics, The Pennsylvania State University,
University Park, PA 16802
E-mail: weiss@math.psu.edu

Submitted: February 18, 2003 *Accepted*: March 9, 2004
Dedicated to Jorge Sotomayor on the occasion of his sixtieth birthday

In this note we explore how simple tools from differential geometry can be used to analyze the behavior of some solutions curves for the Mixmaster universe equation.

Key Words: Mixmaster, Bianchi type IX, Maupertuis principle, negative curvature, geodesics.

1. INTRODUCTION

The Bianchi universes are space-times with spatially locally homogeneous geometry, and thus their gravitational fields are simply functions of time. In these cases the Einstein field equation, a nonlinear partial differential equation, reduces to a system of nonlinear ordinary differential equations. These Bianchi models serve as useful paradigms for studying the nonlinear behavior, and especially the possible chaotic behavior, of the Einstein equations. In particular, these models are useful for investigating the singularities of the evolution of such a universe, where one can study

* This work was partially supported by National Science Foundation grant DMS-0100252. Both authors wish to thank the referee for useful comments.

the behavior of the space-time singularities using methods from the theory of dynamical systems.

The Bianchi IX universe, or Mixmaster universe, is a Bianchi universe with three spacial dimensions. "Mixmaster dynamics" was first investigated by Belinskii, Khalatnikov and Lifshitz [1] and Misner [2]. Simple introductory accounts of this model are given in [3, 4]. If one further assumes the "empty-space condition" or "vacuum cosmology condition," one obtains a space-time metric $ds^2 = -dt^2 + diag(x_1(t), x_2(t), x_3(t))$, where x_1, x_2, and x_3 are solutions of the following system of coupled ordinary differential equations:

$$\begin{aligned}
\frac{x_1''}{x_1} + \frac{x_1'}{x_1}\frac{x_2'}{x_2} + \frac{x_1'}{x_1}\frac{x_3'}{x_3} &= \frac{1}{2(x_1x_2x_3)^2}\left(\left(x_2^2 - x_3^2\right)^2 - x_1^4\right) \\
\frac{x_2''}{x_2} + \frac{x_1'}{x_1}\frac{x_2'}{x_2} + \frac{x_2'}{x_2}\frac{x_3'}{x_3} &= \frac{1}{2(x_1x_2x_3)^2}\left(\left(x_3^2 - x_1^2\right)^2 - x_2^4\right) \\
\frac{x_3''}{x_3} + \frac{x_1'}{x_1}\frac{x_3'}{x_3} + \frac{x_2'}{x_2}\frac{x_3'}{x_3} &= \frac{1}{2(x_1x_2x_3)^2}\left(\left(x_2^2 - x_1^2\right)^2 - x_3^4\right).
\end{aligned} \tag{1}$$

The solutions $x_1 = x_1(t)$, $x_2 = x_2(t)$ and $x_3 = x_3(t)$ determine the *volume* of the universe at time t by $vol(t) = x_1(t) \cdot x_2(t) \cdot x_3(t)$. Since the volume of the universe must be non-negative, solutions with x_1, x_2 or x_3 negative are not considered "physically relevant", and will not considered in this paper.

A *big bang* corresponds to $vol(-t_0) = 0$ and *big crunch* corresponds to $vol(t_1) = 0$ for some solution curve. Clearly the only way for $vol(t)$ to approach 0 is for $\lim_{t_k \to t_0} \min\{x_1(t_k), x_2(t_k), x_3(t_k)\} = 0$, and it is known that this sometimes occurs with *wild* permutations in the directions of the minimum along the sequence.

The system of differential equations is singular when x_1, x_2 or $x_3 = 0$. In particular, the usual existence and uniqueness theorems for solutions of the initial value problem can not be applied at singularities, and little seems to be known about the long-term existence of solutions (up to singularities) [5].

It is well known that system (1) is a Hamiltonian system with Hamiltonian H given by

$$\begin{aligned}
H(x_1, x_2, x_3, x_1', x_2', x_3') &= \frac{x_1'}{x_1}\frac{x_2'}{x_2} + \frac{x_2'}{x_2}\frac{x_3'}{x_3} + \frac{x_3'}{x_3}\frac{x_1'}{x_1} \\
&- \frac{1}{4(x_1x_2x_3)^2}\left(x_1^4 + x_2^4 + x_3^4 - 2(x_1^2x_2^2 + x_2^2x_3^2 + x_1^2x_3^2)\right).
\end{aligned} \tag{2}$$

In the literature, equations (1) and (2) are often rewritten using the parameters $\alpha = \log x_1$, $\beta = \log x_2$ and $\gamma = \log x_3$. One obtains equivalent,

but more concise formulations of (1) and (2) given by

$$\begin{aligned} \ddot{\alpha} &= \frac{1}{2}\left(\left(e^{2\beta}-e^{2\gamma}\right)^2-e^{4\alpha}\right), \\ \ddot{\beta} &= \frac{1}{2}\left(\left(e^{2\gamma}-e^{2\alpha}\right)^2-e^{4\beta}\right), \\ \ddot{\gamma} &= \frac{1}{2}\left(\left(e^{2\alpha}-e^{2\beta}\right)^2-e^{4\gamma}\right), \end{aligned} \tag{3}$$

and

$$H=\dot{\alpha}\dot{\beta}+\dot{\beta}\dot{\gamma}+\dot{\gamma}\dot{\alpha}+\frac{1}{4}\left(e^{2\alpha}+e^{2\beta}+e^{2\gamma})^2-2(e^{4\alpha}+e^{4\beta}+e^{4\gamma})\right). \tag{4}$$

Here we understand $(\dot{\ })=\frac{d}{d\tau}=(x_1x_2x_3)\frac{d}{dt}$ and $(\ddot{\ })=\frac{d^2}{d\tau^2}=(x_1x_2x_3)^2\frac{d^2}{dt^2}+(x_1x_2x_3)(x_1'x_2x_3+x_1x_2'x_3+x_1x_2x_3')\frac{d}{dt}$. This equivalent system is a system of regular ordinary differential equations.

The aim of this note is to apply simple tools in differential geometry to analyze some qualitative features of certain solution curves to (1) in certain regions. Since (1) is a Hamiltonian system, we can apply the Maupertius Principle, and thus after a suitable time parametrization, some trajectories can be interpreted as geodesics for a suitable metric on a subset of $\mathbb{R}^3$. Since the kinetic energy is not positive definite, formally, one needs to apply a generalized version of the Maupertuis Principle. Properties of the metric, such as curvature, determine important qualitative features of the solution curves. Although this approach is limited to studying solutions curves in regions where the hypothesis of the Maupertuis Principle are satisfied (where the potential for the associated Lagrangian is negative), it is particularly interesting in two respects:

(i) The explicitly computable Christoffel symbols provide simple qualitative descriptions of how the associated geodesics, and thus the solutions to (1), evolve.

(ii) The regions where the geometric picture applies, and where the Christoffel symbols (and sectional curvatures) attain different values are particularly beautiful in structure; their appearance provide insights into the highly complicated and subtle behavior of some solutions to (1).

2. QUALITATIVE FEATURES

We begin by recalling some well known general observations.

LEMMA 1. *When α, β, and γ are all very negative, the solutions of (3) are close to linear.*

Proof. By inspection, when α, β, and γ are all very negative the equations (3) are approximated by $\alpha'' = \beta'' = \gamma'' = 0$. The solutions of these three equations are linear functions. ∎

We now show that the volume is convex function along zero-energy solution curves.

LEMMA 2. *When $H = 0$, the* (log) *volume function $-\log vol(t)$ is a convex function of t.*

Proof. Adding the three equations in (1) we have that

$$\begin{aligned}\frac{x_1''}{x_1} + \frac{x_2''}{x_2} + \frac{x_3''}{x_3} &= \frac{\left(x_1^4 + x_2^4 + x_3^4 - 2(x_1^2x_2^2 + x_2^2x_3^2 + x_1^2x_3^2)\right)}{2(x_1x_2x_3)^2} \\ &\quad - 2\left(\frac{x_1'}{x_1}\frac{x_2'}{x_2} + \frac{x_2'}{x_2}\frac{x_3'}{x_3} + \frac{x_3'}{x_3}\frac{x_1'}{x_1}\right) \\ &= 0, \quad \text{using (2).}\end{aligned}$$

We can then write

$$\frac{d^2}{dt^2}\log vol(x_1x_2x_3) = \frac{x_1''}{x_1} + \frac{x_2''}{x_2} + \frac{x_3''}{x_3} - \left[\left(\frac{x_1'}{x_1}\right)^2 + \left(\frac{x_2'}{x_2}\right)^2 + \left(\frac{x_3'}{x_3}\right)^2\right] \leq 0.$$

In particular, we see that $\log vol(x_1x_2x_3)$ increases monotonically to a unique maximum and decreases monotonically, and thus the same for the product $x_1x_2x_3$. ∎

The following corollary follows immediately from the convexity of volume.

COROLLARY 3. *One of the following three scenarios must occur:*

(i) *The volume $vol(t)$ starts from zero at time t_0, increases monotonically to a unique maximum, and decreases monotonically to zero at time t_1;*

(ii) *The volume $vol(t)$ starts from zero at time t_0 and increases without bound as $t \to +\infty$;*

(iii) *The volume $vol(t)$ starts from zero at time t_0 and increases to a finite limiting value as $t \to +\infty$;*

Besides the obvious physical significance, this lemma is also helpful when interpreting numerical approximations, which we call numerical solutions, to (1) and (3). Here one only needs to consider solution curves defined on (t_0, t_1), where $t_0 < 0 < t_1$ such that $vol(t_0) = 0 = vol(t_1)$ and $vol(t)$ is

strictly positive for intermediate values $t \in (t_0, t_1)$. Although the actual solutions are singular at t_0 and t_1, the numerical solutions may seem to exist on a larger time interval, and this extra piece of solution may be discarded.

Example. Consider the solution of equation (1) with initial point $(x_1(0), x_2(0), x_3(0)) = (1, 4, 1)$ and initial vector $(x_1'(0), x_2'(0), x_3'(0)) = (0, 1, -15.75)$. The value of $x_3'(0)$ was chosen after the other five values to ensure that $H = 0$. Figure 1 contains a Mathematica plot of a numerical solution in the range $t_0 < t < t_1$, where $t_0 = -85$ and $t_1 = 0.065$. We shall want to concentrate on the orbit segment in the range $t_2 < t < t_3$, where $t_2 = -1.4$ and $t_3 = -0.45$ (see Figure 2), for on this range the orbit can be interpreted as a geodesic (see Section 3). We will return to this example several times throughout the paper.

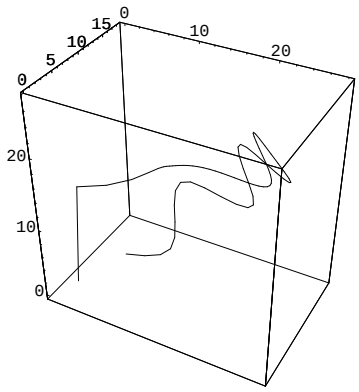

FIG. 1. The full orbit with parameter $t_0 < t < t_1$ for $t_0 = -85$ and $t_1 = 0.065$.

3. METRICS AND GEODESIC FLOWS

There are various ways one can try to analyze such a complicated system of differential equations as (1). The corresponding dynamical system seems far from any of the well-studied classes, e.g., Morse-Smale flows, hyperbolic flows, etc. In this note we adopt a geometric viewpoint. More precisely, the solutions to (1) arise from a Hamiltonian flow, which by a suitable parametrization, can be reinterpreted as a geodesic flow for a suitable metric on a subset of $\mathbb{R}^3$.

The following simple proposition illustrates how geometry effects the behavior of geodesic curves, in the simpler case of a geodesic flow on a surface.

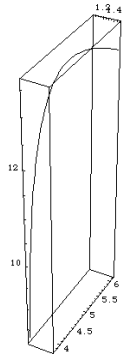

FIG. 2. Part of the orbit in the range $t_2 < t < t_3$.

PROPOSITION 4. *Consider an open subset U of $\mathbb{R}^2$ with a Riemannian metric $ds^2 = Edx_1^2 + 2Fdx_1dx_2 + Gdx_2^2$.*

(i) *The local behavior of a geodesic γ is explicitly determined by the Christoffel symbols, and is only implicitly determined by the curvature.*

(ii) *If the surface has negative curvature in an open set U containing p, then the geodesic flow exhibits sensitive dependence on initial conditions in U.*

Proof. A geodesic γ is a solution of the following system of differential equations

$$\begin{aligned}
\frac{d^2\gamma^{(1)}}{ds^2} &= \Gamma^1_{11}\left(\frac{d\gamma^{(1)}}{ds}\right)^2 + 2\Gamma^1_{12}\frac{d\gamma^{(1)}}{ds}\frac{d\gamma^{(2)}}{ds} + \Gamma^1_{22}\left(\frac{d\gamma^{(2)}}{ds}\right)^2 \\
\frac{d^2\gamma^{(2)}}{ds^2} &= \Gamma^2_{11}\left(\frac{d\gamma^{(1)}}{ds}\right)^2 + 2\Gamma^2_{12}\frac{d\gamma^{(1)}}{ds}\frac{d\gamma^{(2)}}{ds} + \Gamma^2_{22}\left(\frac{d\gamma^{(2)}}{ds}\right)^2.
\end{aligned}$$

If we assume, without loss of generality, that local coordinates are chosen near a point such that at the point $\frac{d\gamma}{ds} = (1, 0)$, then this system of differential equations reduces to

$$\frac{d^2\gamma^{(1)}}{ds^2} = \Gamma^1_{11} \quad \text{and} \quad \frac{d^2\gamma^{(2)}}{ds^2} = \Gamma^2_{11}.$$

Intuitively, the geodesic "bends to the left" if $\Gamma^1_{11} < 0$ and "bends to the right" if $\Gamma^2_{11} < 0$. The curvature is given by the more complicated

expression

$$\kappa = (1/E)(\Gamma^2_{11} - \Gamma^2_{12} + \Gamma^2_{12}(\Gamma^1_{11} - \Gamma^2_{12}) + \Gamma^2_{12}(\Gamma^1_{11} - \Gamma^2_{12})),$$

and there is no simple connection between the nature of γ and κ, although they are implicitly related.

By contrast the curvature directly effects the parallel Jacobi fields for γ. Following the standard proof (via the Riccati equation) [6], one sees that negative curvature causes (local) exponential growth of most parallel Jacobi fields, which we interpret as sensitive dependence on initial conditions. ▌

Geometry in three dimensions is more complicated than in two dimensions and requires more sophisticated geometric analysis. For instance, in dimension three there are, before symmetries, 27 Christoffel symbols, while in dimension two there are only 8 Christoffel symbols.

Starting with the Hamiltonian H, we consider the potential

$$V(x_1, x_2, x_3) = -\frac{1}{4(x_1x_2x_3)^2}\left((x_1^4 + x_2^4 + x_3^4) - 2(x_1^2x_2^2 + x_2^2x_3^2 + x_1^2x_3^2)\right)$$

$$= -\frac{1}{4(x_1x_2x_3)^2}(x_1 + x_2 - x_3)(x_1 + x_2 + x_3)(x_1 + x_3 - x_2)(x_1 - x_2 - x_3),$$

or equivalently, $V(\alpha, \beta, \gamma) = \frac{1}{4}\left(e^{2\alpha} + e^{2\beta} + e^{2\gamma}\right)^2 - 2\left(e^{4\alpha} + e^{4\beta} + e^{4\gamma}\right)$. From these expressions for V one immediately sees that the algebraic variety $\{V = 0\}$ is the union of four planes and is invariant under the group of symmetries of the cube centered at the origin.

The associated Lagrangian $L = H - V$ on $T\mathbb{R}^3 = \mathbb{R}^6$ takes the form

$$L(q, v) = (v_1v_2 + v_2v_3 + v_3v_1) - V(q),$$

where $q = (\alpha, \beta, \gamma)$. We assume that the energy E of the system is zero, [1] and define the metric

$$ds^2 = -V(q)\left(dx_1dx_2 + dx_2dx_3 + dx_3dx_1\right),$$

whenever $V(q) < 0$.

In matrix notation we get

$$(g_{ij}) = V\begin{pmatrix} 0 & \frac{1}{2} & \frac{1}{2} \\ \frac{1}{2} & 0 & \frac{1}{2} \\ \frac{1}{2} & \frac{1}{2} & 0 \end{pmatrix} \quad \text{and} \quad (g^{ij}) = -\frac{1}{V}\begin{pmatrix} -1 & 1 & 1 \\ 1 & -1 & 1 \\ 1 & 1 & -1 \end{pmatrix}.$$

This metric is non-degenerate and symmetric, but is not Riemannian. In the region where $V(q) < 0$, the matrix (g_{ij}) has index two (two negative eigenvalues). However, much of the theory of Riemannian geometry

[1] Some authors relax this hypothesis and assume that the energy $E \neq 0$ [7].

carries over directly to non-Riemannian metrics [8]. The relation between geodesics of the metric and solutions of (1) is given by the following classical result.

PROPOSITION 5. *(Maupertuis Principle) [9, 10] On the subset $W \subset \mathbb{R}^3$ where $-V(q) > 0$, the solutions to (1) are reparameterized geodesics $\gamma(t) = (\gamma^{(1)}(t), \gamma^{(2)}(t), \gamma^{(3)}(t))$ for the metric (g_{ij}).*

The region of definition of the metric is the semi-algebraic set W

$$\begin{aligned} W &= \{(x_1, x_2, x_3) : \ -V(x_1, x_2, x_2) > 0\} \\ &= \{(x_1, x_2, x_3) : x_1^4 + x_2^4 + x_3^4 > 2(x_1^2x_2^2 + x_2^2x_3^2 + x_1^2x_3^2)\}. \end{aligned}$$

The region W is clearly symmetric under permutation of the axes and does not contain the origin. Solutions to (1) may exist outside of W, but they lose their interpretation as geodesics. One can easily check the following facts.

LEMMA 6.

(a) *The set W does not intersect the diagonal $D = \{(x_1, x_1, x_1)\}$[2]; and*
(b) *The set W is disjoint from the faces of the positive quadrant.*

We can try to visualize the function $V(x_1, x_2, x_3)$ by considering cross sections in the x_1x_2-plane for fixed values of x_3. In Figure 3, we present both the three dimensional plots and density plots of the three sections $V(x_1, x_2, 2)$, $V(x_1, x_2, 4)$ and $V(x_1, x_2, 6)$ for $0 \le x_1, x_2 \le 10$.

Example revisited. In the example we described in the previous section, one can easily check that $V(1, 4, 1) = -3.3975 < 0$, so that the solution is, at least initially, in the domain W of interest. To help study the orbit in W, we plot the potential function V along the orbit, and we obtain the plot shown in Figure 4. In particular, we observe that the restriction to the range $t_2 < t < t_3$, where $t_2 = -1.4$ and $t_3 = -0.45$ gives $V(t) < 0$, and thus this portion of the orbit corresponding to a geodesic.

The geodesics $\gamma(t) = (\gamma^{(1)}(t), \gamma^{(2)}(t), \gamma^{(3)}(t))$ for the metric ds^2 are solutions of the system of differential equations

$$\frac{d^2\gamma^{(k)}}{dt^2} + \sum_{i,j=1}^{3} \Gamma_{ij}^k \frac{d\gamma^{(i)}}{dt} \frac{d\gamma^{(j)}}{dt} = 0,$$

[2]Although, when $E < 0$ the set W intersects the diagonal D in the set $\{(x_1, x_1, x_1) : x_1 \in (0, 3/\sqrt{2|E|})\}$, and for $E \ge 0$ the set W is disjoint from the diagonal.

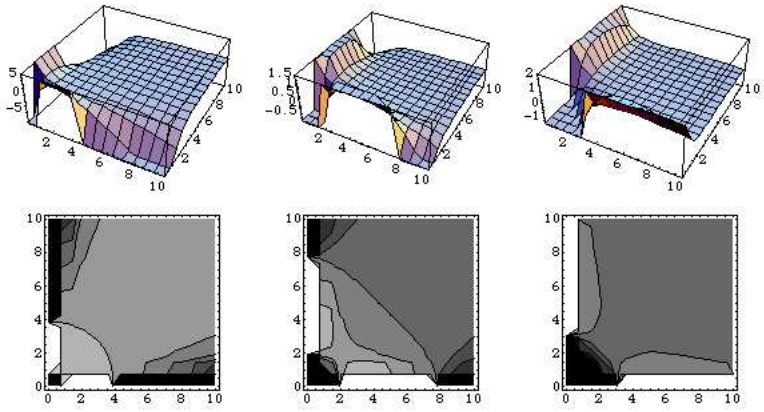

FIG. 3. Three cross sections of values for the function V.

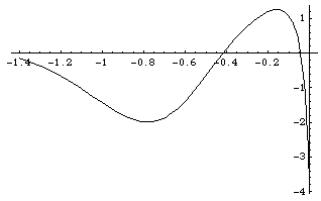

FIG. 4. The value of the function V along the orbit.

where Γ_{ij}^k is the Christoffel symbol defined by

$$\Gamma_{ij}^k = \frac{1}{2}\sum_{l=1}^{3} g^{kl}\left(\frac{\partial g_{lj}}{\partial x_i} + \frac{\partial g_{li}}{\partial x_j} - \frac{\partial g_{ij}}{\partial x_l}\right). \tag{5}$$

The relationship between the naturally parameterized solution curves to (1) and the geodesics can be immediately seen from the definition of the metric. In particular, the reparameterization of the geodesics tends to infinity as $(-V) \to 0$. This corresponds to the singularities that occur in the solution curves for (1).

4. CHRISTOFFEL SYMBOLS AND THE BEHAVIOR OF SOLUTIONS

We already observed that when α, β, γ are small the solutions of (3) are close to linear. A more refined analysis of the equations for the geodesic flow reveals more on the eccentric behavior of the orbits.

We see from the definitions that $g_{ij} = \frac{1}{2}(1-\delta_{ij})(-V)$ and the inverse $(g^{ij}) = (1-2\delta_{ij})(-V)^{-1}$. The derivatives

$$\begin{aligned} \frac{\partial g_{lk}}{\partial x_j} &= \frac{1}{2}(1-\delta_{lk})\frac{\partial(-V)}{\partial x_j} \quad \text{and} \\ \frac{\partial(-V)}{\partial x_j} &= \frac{2V}{x_j} + \frac{x_j(2x_j^2 - R^2)}{(x_1x_2x_3)^2}, \end{aligned}$$

where $R^2 = x_1^2 + x_2^2 + x_3^2$. Then the Christoffel symbols (5) are given by the following explicit expressions:

$$\begin{aligned} \Gamma_{ij}^k &= \frac{1}{2(-V))}\sum_{l=1}^{3}(1-2\delta_{kl})\left(\frac{\partial g_{li}}{\partial x_i} + \frac{\partial g_{lj}}{\partial x_j} - \frac{\partial g_{ij}}{\partial x_l}\right) \\ &= \frac{1}{2(-V)}\left(\sum_{l=1}^{3}(1-2\delta_{kl})(1-\delta_{lj})\frac{\partial(-V)}{\partial x_i} + \sum_{l=1}^{3}(1-2\delta_{kl})(1-\delta_{li})\frac{\partial(-V)}{\partial x_j}\right. \\ &\qquad \left. - \sum_{l=1}^{3}(1-2\delta_{kl})(1-\delta_{ij})\frac{\partial(-V)}{\partial x_l}\right) \\ &= \frac{1}{2(-V)}\left(\frac{\partial(-V)}{\partial x_i}\sum_{l=1}^{3}(1-2\delta_{kl})(1-\delta_{lj}) + \frac{\partial(-V)}{\partial x_j}\sum_{l=1}^{3}(1-2\delta_{kl})(1-\delta_{li})\right. \\ &\qquad \left. - (1-\delta_{ij})\sum_{l=1}^{3}(1-2\delta_{kl})\frac{\partial(-V)}{\partial x_l}\right) \\ &= \frac{1}{2(-V)}\left(\frac{\partial(-V)}{\partial x_i}\delta_{kj} + \frac{\partial(-V)}{\partial x_i}\delta_{ki} - \frac{1}{2}(1-\delta_{ij})\sum_{l=1}^{3}(1-2\delta_{kl})\frac{\partial(-V)}{\partial x_l}\right) \\ &= \frac{1}{2(-V)}\left(\delta_{kj}\left(\frac{x_i(2x_i^2-R^2)}{(x_1x_2x_3)^2} + \frac{2V}{x_i}\right) + \delta_{ki}\left(\frac{x_j(2x_j^2-R^2)}{(x_1x_2x_3)^2} + \frac{2V}{x_j}\right)\right. \\ &\qquad \left. - \frac{1}{2}(1-\delta_{ij})\sum_{l=1}^{3}(1-2\delta_{kl})\left(\frac{x_l(2x_i^2-R^2)}{(x_1x_2x_3)^2} + \frac{2V}{x_l}\right)\right). \end{aligned}$$

Christoffel symbols always have the symmetry $\Gamma_{ij}^k = \Gamma_{ji}^k$. Looking at the denominators in this expression, it is immediate that the geodesics, and thus the solution curves of (1), tend to bend more rapidly

1. as $V \to 0$; or
2. as x_1, x_2, or $x_3 \to 0$.

In this case it is the sign of the Γ_{ij}^k which determines the directions in which the geodesic bends. This is easily determined using the formula

above. For example, if $\dot{\gamma}(0) = (v_1, v_2, v_3) \in \mathbb{R}^3$, then the pull in the x_1-direction, say, is determined by $(d^2\gamma^{(1)}/ds^2)(0) = \langle (d^2\gamma/ds^2)(0), (1,0,0)\rangle$, and thus the sign of

$$(d^2\gamma^{(1)}/ds^2)(0) = \sum_{i,j=1}^{3} \Gamma^1_{ij} v_i v_j. \tag{6}$$

To complete this section, we apply our general geometric principle in a few simple cases.

PROPOSITION 7. *(Application of geometric principle)*

Case 1. *Assume that the geodesic is directed along the diagonal. In particular,* $\gamma^{(1)}(0) = \gamma^{(2)}(0) = \gamma^{(3)}(0)$ *and* $(d\gamma^{(1)}/dt)(0) = (d\gamma^{(2)}/dt)(0) = (d\gamma^{(3)}/dt)(0)$. *An easy calculation shows that for each fixed* $k = 1, 2$ *or* 3, *the Christoffel symbols sum to zero, and we deduce from (6) that*

$$\frac{d^2\gamma^{(1)}}{dt^2}(0) = \frac{d^2\gamma^{(2)}}{dt^2}(0) = \frac{d^2\gamma^{(3)}}{dt^2}(0).$$

Thus the geodesic initially proceeds along the diagonal. [3]

Case 2. *Assume that the geodesic is initially directed parallel to the* x_3*-axis. Then* $(d\gamma^{(3)}/dt)(0) = 1$ *and* $(d\gamma^{(1)}/dt)(0) = (d\gamma^{(2)}/dt)(0) = 0$ *and then (1.1) reduces to*

$$\frac{d^2\gamma^{(1)}}{dt^2}(0) = \Gamma^1_{33}(0) = 0 \quad \text{and} \quad \frac{d^2\gamma^{(2)}}{dt^2}(0) = \Gamma^2_{33}(0) = 0,$$

and the geodesic initially proceeds along a straight line.

Case 3. *Let us consider the case where* $x_1(0) >> x_2(0) >> x_3(0)$. *In particular, the initial point is closest to the* x_1x_2*-plane. Then the Christoffel symbols satisfy*

$$\begin{aligned}
\Gamma^3_{12} &\sim 1/(2x_3) + O(1/(2x_2), x_1/Vx_2^2x_3^2)\\
\Gamma^3_{13} &\sim 1/(2x_3) + O(1/(2x_2), x_1/Vx_2^2x_3^2)\\
\Gamma^3_{23} &\sim 1/(2x_3) + O(1/(2x_2), x_2/Vx_1^2x_3^2).
\end{aligned}$$

For example, when $(x_1, x_2, x_3) = (100, 10, 1)$, *we have that* $\Gamma^3_{12} = -0.453346$. *When* $(x_1, x_2, x_3) = (10000, 100, 1)$, *we have that* $\Gamma^3_{12} = -0.495048$. *If for*

[3] The referee pointed out that "along the diagonal" the system of differential equations (1) with $x_k(t) = x(t), k = 1, 2, 3$ reduces to the scaler equation $xx'' + 2x'^2 = -1/2$. As long as $x(0) \neq 0$, a solution of the initial value problem exists, which means that the solution continues along the diagonal.

a geodesic γ, $\gamma(0)$ is in the positive quadrant and γ heads toward the x_1x_2-plane, then the principal terms dominate, and thus $(d^2\gamma^{(3)}/ds^2)(0) < 0$, i.e., the geodesic is deflected away from the plane.

5. CURVATURE AND SENSITIVE DEPENDENCE ON INITIAL CONDITIONS

The curvature of the region W with respect to these metrics has been studied by Aizawa, Koguro and Antoniou in [12]. We refer there for a discussion of the behavior of the sectional curvatures across the space. However, instead of studying the behavior of a single geodesic, we can take our lead from the theory of Anosov systems and consider families of nearby geodesics, so that we can consider the instability of these orbits. In particular, the behavior of nearby orbits is directly influenced by the behavior of Jacobi fields, and thus in turn explicitly by the curvature.

We can express the curvature in terms of Christoffel symbols

$$R^s_{ijk} = \sum_{l=1}^{3} \Gamma^l_{ik}\Gamma^s_{jl} - \sum_{l=1}^{3} \Gamma^l_{jk}\Gamma^s_{il} + \frac{\partial}{\partial x_j}\Gamma^s_{ik} - \frac{\partial}{\partial x_i}\Gamma^s_{jk}$$

and

$$\langle R(X_i, X_j)X_k, X_s\rangle = R_{ijks} := \sum_{l=1}^{3} R^l_{ijk}g_{ls}.$$

We define the *sectional curvature* relative to the plane spanned by $v = (v_1, v_2, v_3)$ and $w = (w_1, w_2, w_3)$ by

$$\kappa(v, w) = \frac{\sum_{i,j=1}^{3} v_i w_j R_{ijij}}{|v \wedge w|^2}$$

We associate to a given geodesic γ parallel Jacobi fields. These should satisfy the Jacobi equation

$$Y'' + RY = 0.$$

We can rewrite this is coordinate form

$$\frac{d^2y_m}{ds^2} + \sum_{i,j=1}^{3} R^m_{ijk}\frac{d\gamma^{(i)}}{ds}y_j\frac{d\gamma^{(k)}}{ds} = 0.$$

The sectional curvatures are important in describing the oscillation in the orbits, as is summarized in the following simple result.

PROPOSITION 8. *Given a geodesic $\gamma : \mathbb{R} \to \mathbb{R}^3$, choose a parallel Jacobi field $Y(t)$, and consider the 2-dimensional plane span$\{\dot\gamma(0), Y(0)\}$ $(i = 1, 2)$.*

(i) *If the sectional curvature in the plane span $\{\dot\gamma(0), Y_i(0)\}$ is negative, then the orbits start to diverge exponentially fast in that plane.*

(ii) *If the sectional curvature in the plane span $\{\dot\gamma(0), Y_i(0)\}$ is positive, then the orbits tend to start oscillating in that plane.*

Proof. It follows from the standard proof of geodesic flows on negatively curved manifolds being Anosov [11] that most solutions $Y(t)$ grow exponentially in t. This gives the exponential divergence of nearby orbits in part (i).

In the case that the sectional curvature in the plane is positive, it is well known that the Jacobi field tends to oscillate, leading to part (ii). ▌

Example Revisited. We can illustrate the instability of nearby orbits by considering our simple example. Let us consider a second orbit starting from the same initial value $(x_1(0), x_2(0), x_3(0)) = (1, 4, 1)$, but having a very slightly different initial derivative vector: $(x_1'(0), x_2'(0), x_3'(0)) = (0, 1.1, -14.3181\ldots)$. In Figure 5 we plot both the orbit segment for the original trajectory and this perturbed trajectory in the range $t_2 < t < t_3$.

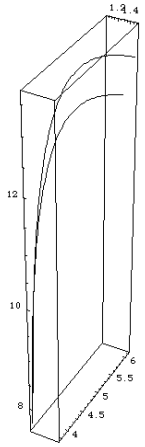

FIG. 5. Two orbits with the same initial point exhibiting a rapid divergence of their orbits.

Remark. We have not directly considered the case of $x_1(0) << x_2(0) << x_3(0)$, say, where one obtains the "Kasner solutions" (cf. [3] for a nice account). These special solutions are approximated by an exponential curve

for $x_3(t)$ and oscillating curves in $x_1(t)$ and $x_2(t)$. Moreover, in the Kasner solutions, at various times, the relative magnitudes of the functions $x_1(0), x_2(0), x_3(0)$ may change and the rôle of the oscillating and decreasing solutions interchange (at least for a finite number of instances). This leads to the Kasner cycles and periods, and the change over is approximated using analysis of the CFT [3, 13]. This phenomena may well occur outside of the region to which the above analysis applies.

REFERENCES

1. V. Belinskii, I. Khalatnikov, and E. Lifschitz, *Oscillatory Approach to the Singular Point in the Relativistic Cosmology*, Advances in Physics **19** (1970), 525–573.
2. C. Misner, *Chaotic Behaviour in General Relativity*, Physics Reports **85** (1982), 1–49.
3. J. Barrow, *The Mixmaster Universe*, Phys. Rev. Letters **22** (1969), 1071–1071.
4. S. Rugh, *Chaos in the Einstein Equations – Characterizations and Importance*, Deterministic Chaos in General Relativity (1992), 359–422.
5. A. Rendall, *Theorems on Existence and Global Dynamics for the Einstein Equations*, Living Reviews in Relativity **5** (2002), http://relativity.livingreviews.org/Articles/lrr-2002-6/index.html.
6. W. Klingenberg, *Riemannian Geometry*, Walter de Gruyter (1982).
7. S. Rugh, *Chaotic Behaviour and Oscillating Three-volumes in Bianchi IX Universes*, Physics letters A (1990), 353–359.
8. B. O'Neill, *Semi-Riemannian Geometry*, Academic Press (1983).
9. V. Arnold, *Mathematical Methods of Classical Mechanics*, Springer Verlag (1989).
10. S. Rugh, *Maupertuis Principle, Wheeler's Superspace and an Invariant Criterion for Local Instability in General Relativity*, preprint.
11. D. Anosov, *Geodesic Flows on Closed Riemann Manifolds with Negative Curvature*, Proceedings of the Steklov Institute of Mathematics,**90** (1967).
12. Y. Aizawa, N. Koguro and I. Antoniou, *Chaos and Singularities in the Mixmaster Universe*, Progress of Theoretical Physics (1997), 1225-1250.
13. Y. Manin and M. Marcolli, *Continued Fractions, Modular Symbols, and Noncommutative Geometry*, Selecta Math. (2002), 475–521.